

MOF/polymer composite synthesized using a double solvent method offers enhanced water and CO₂ adsorption properties

Li Peng, Shuliang Yang, Daniel T. Sun, Mehrdad Asgari, Wendy L. Queen*

Institut des Sciences et Ingénierie Chimiques, École Polytechnique Fédérale de Lausanne (EPFL) - Valais Wallis, CH-1951 Sion, Switzerland.

E-mail: wendy.queen@epfl.ch

1. Materials, Experimental process and Calculation information

Materials. Nickel(II) acetate tetrahydrate (98+%) were obtained from Alfa Aesar. 4,4'-benzene-1,4-diylbis(1*H*-pyrazole) was provided by Aromalake. Dopamine hydrochloride, anhydrous methanol and Magnesium acetate were purchased from Sigma. Anhydrous hexane was purchased from TCI. Ammonium hydroxide (25% NH₃) was produced by ABCR. DMF was obtained from Roth AG. All chemicals were used as received without any further purification. Water used in all experiments was deionized.

Ni-MOF synthesis. Ni-MOF was synthesized according to the literature. In a typical synthesis, 63 mg of 4,4'-benzene-1,4-diylbis(1*H*-pyrazole) was dissolved in 16 mL of DMF and 100 mg of Ni(OAc)₂·4H₂O was dissolved in 4 mL of H₂O. The two solutions were mixed together and refluxed for 6 h under stirring. The solid was filtered and washed with EtOH and Et₂O. Then this solid was soxhleted with CH₂Cl₂ for 7 hours. After drying the Ni-MOF was obtained.

Ni-MOF/PDA composites synthesis. First, the Ni-MOF powder (130 mg) was heated at 130 °C under vacuum for 7 h. Then, 10 mL anhydrous hexane was injected into the powder and stirred for 30 min. After that different amount of dopamine hydrochloride (for Ni-MOF/PDA-1: 28 mg, Ni-MOF/PDA-2: 56 mg, Ni-MOF/PDA-3: 112 mg) dissolved in 288 μL water was added into the reactor. The mixture was stirred for one hour and the solution was poured away and only the solid left in the bottle. Then 20 mL EtOH, 45 mL H₂O and 375 μL NH₃·H₂O were added into the solid and stirred for 9 hours. (Note: when the reaction was running, a needle was put in the rubber stopper to connect the reaction system with air.) Finally, the resulting product was soxhleted with methanol and was dried overnight at room temperature.

Ni-MOF-PDA-4 composites synthesis. First, the Ni-MOF powder (130 mg) was heated at 130 °C under vacuum for 7 h. Dopamine hydrochloride 112 mg dissolved in 288 μL water was added into 20

mL EtOH, 45 mL H₂O and 375 μ L NH₃·H₂O were added into the solid and stirred for 9 hours. Finally, the resulting product was washed with methanol and was dried overnight at room temperature.

Synthesis of Ni-MOF/PDA-Mg: 35 mL methanol was added into 130 mg Ni-MOF/PDA-2 and the solution was ultrasonicated for few seconds. Then 75 mg Magnesium acetate was added into the solution and stirred for 12 hours. The obtained solid was washed with methanol and dried under vacuum.

Characterization. The morphologies of the materials were characterized by scanning electron microscopy (FEI Teneo SEM). Synchrotron radiation powder X-ray diffraction data was collected at the BM02 (D2am French CRG beamline) at the European Synchrotron Radiation Facility (ESRF in Grenoble, France) using a XPAD3 hybrid pixel detector. The wavelength used in different experiments was 0.5635645 Å, and the sample to detector distance was 400 mm. All parameters required for integration were calibrated using a standard LaB6 sample. The porosity properties were gained from nitrogen adsorption-desorption isotherms using BELSORP-max instrument. The loading content of Mg was determined by Agilent 5110 Synchronous Vertical Dual View ICP-OES. The IR data was obtained on PerkinElmer Frontier Spectrometer.

Determination of Isothermic heats,¹⁻³-Q_{st}:

The CO₂ adsorption isotherms collected at 288 K, 298 K and 308 K were fitted with a dual-site Langmuir model (Eqn. 1) as following:

$$n = \frac{q_{\text{sat},1} b_1 P}{1 + b_1 P} + \frac{q_{\text{sat},2} b_2 P}{1 + b_2 P} \quad (1)$$

where n is the amount adsorbed in mmol/g, q_{sat,1} is the adsorption capacity for site I, b₁ is the Langmuir parameter, and P is the pressure in mbar. The fitted parameters for each adsorption isotherm can be found in Table S2. The comparison of the experimental CO₂ adsorption isotherms with the fitted dual-site Langmuir model based on the experimental data are shown in the Figure S4. Then the Clausius-Clapeyron equation (Eqn. 2) was subsequently used to calculate the isosteric heats of adsorption, Q_{st}, for CO₂ in each analog, using the dual-site Langmuir-Freundlich fits for each material at 288 K, 298 K, and 308 K, to calculate the pressures that correspond to a given CO₂ loading at each temperature.

$$\ln P = -\frac{Q_{st}}{R} \left(\frac{1}{T} \right) + C \quad (2)$$

Here, P is the pressure, n is the amount adsorbed, T is the temperature, R is the universal gas constant, and C is a constant. The isosteric heat of adsorption, Q_{st} , was obtained from the slope of plots of $(\ln P)_n$ as a function of $1/T$. An error in the isosteric heat for a given loading can be calculated from the standard error in slope of the best-fit line. Fundamentally, this error describes the quality of agreement between the fitted isotherms and the Clausius-Clapeyron relation.

Selectivity calculation:

The following equation has been used to obtain the selectivity⁴:

$$S = \frac{q_{CO_2}|_{P_{CO_2}}}{q_{N_2}|_{P_{N_2}}} * \frac{P_{N_2}}{P_{CO_2}}$$

Where $q_{CO_2}|_{P_{CO_2}}$ is the adsorption amount of CO_2 under the corresponding CO_2 partial pressure, $q_{N_2}|_{P_{N_2}}$ is the adsorption amount of N_2 under the corresponding N_2 partial pressure, and P_{CO_2} and P_{N_2} are partial pressure of CO_2 and N_2 in post combustion capture application. In order to better assess the selectivity, the values of $q_{CO_2}|_{P_{CO_2}}$ and $q_{N_2}|_{P_{N_2}}$ has been obtained using a developed python package⁵ of Ideal Adsorption Solution Theory (IAST) which simulates the adsorption amount of an adsorbent material in multicomponent stream by using single component adsorption isotherms for each individual component.

2. Characterization data

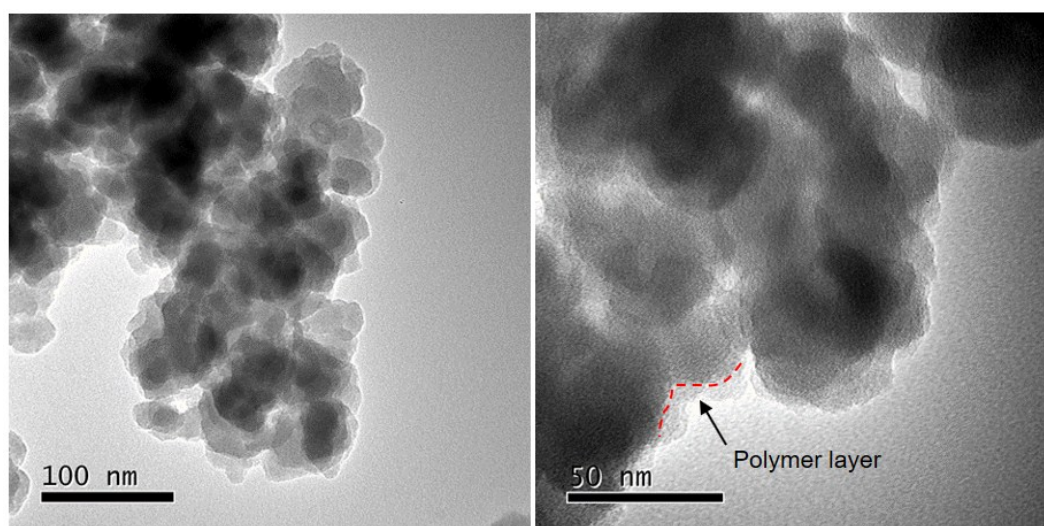


Fig. S1 TEM images of as-synthesized Ni-MOF-PDA-4.

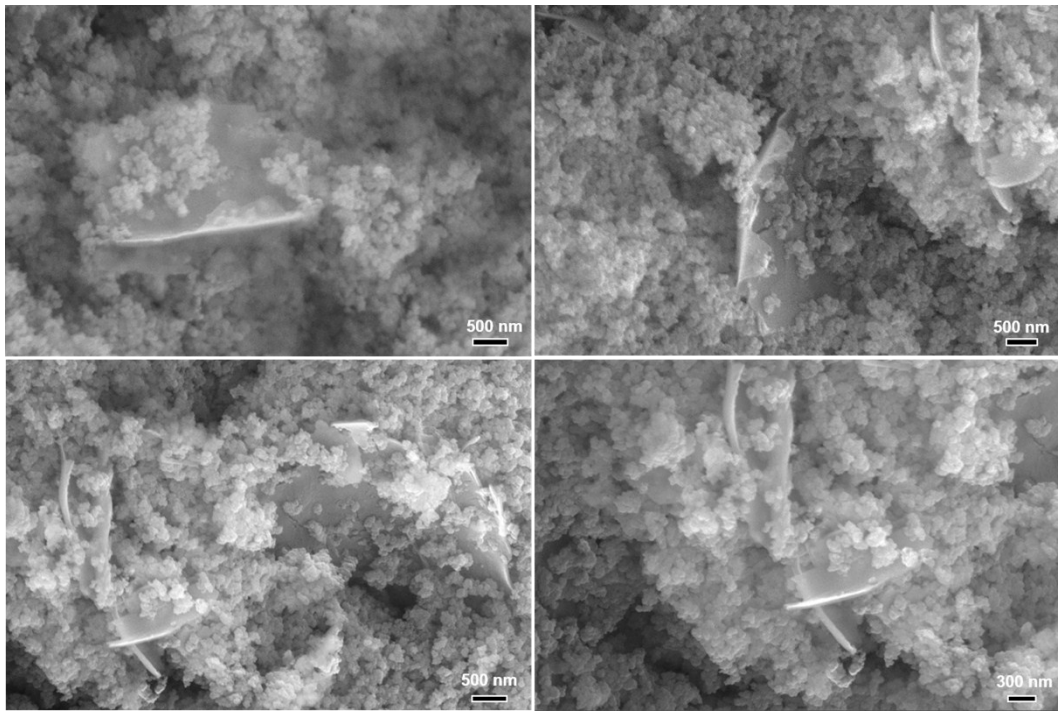
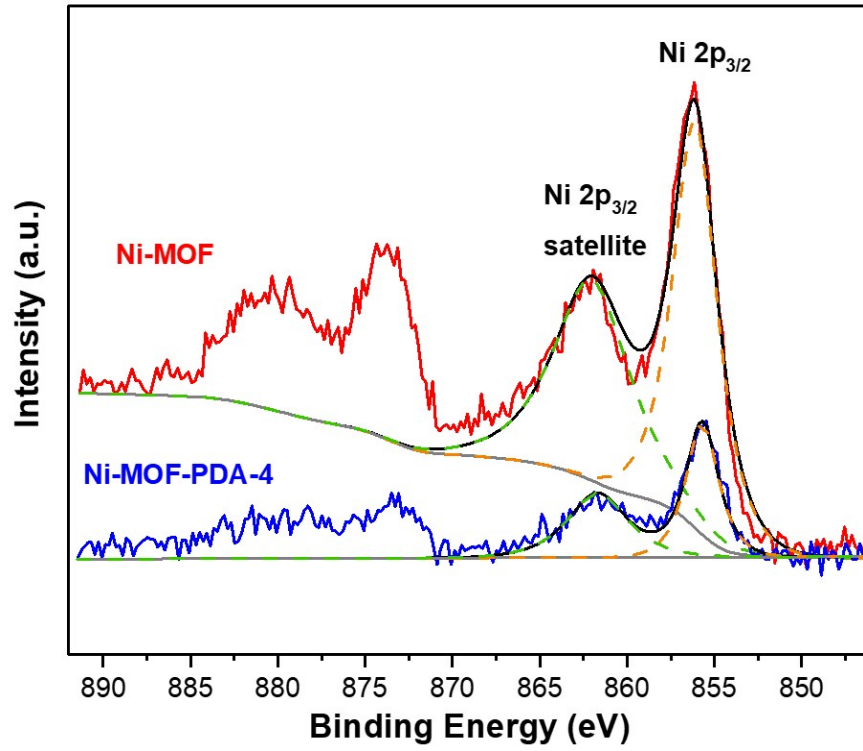


Fig. S2 SEM images of as-synthesized Ni-MOF-PDA-4.



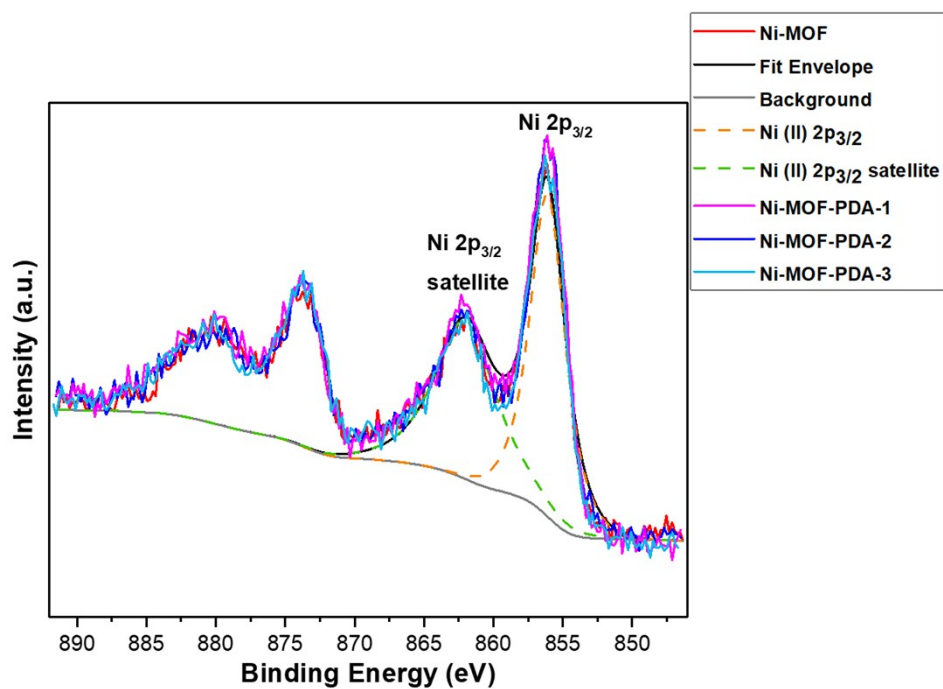


Fig. S3 XPS spectra of Ni 2p of Ni-MOF, Ni-MOF-PDA-1, Ni-MOF-PDA-2, Ni-MOF-PDA-3 and Ni-MOF-PDA-4.

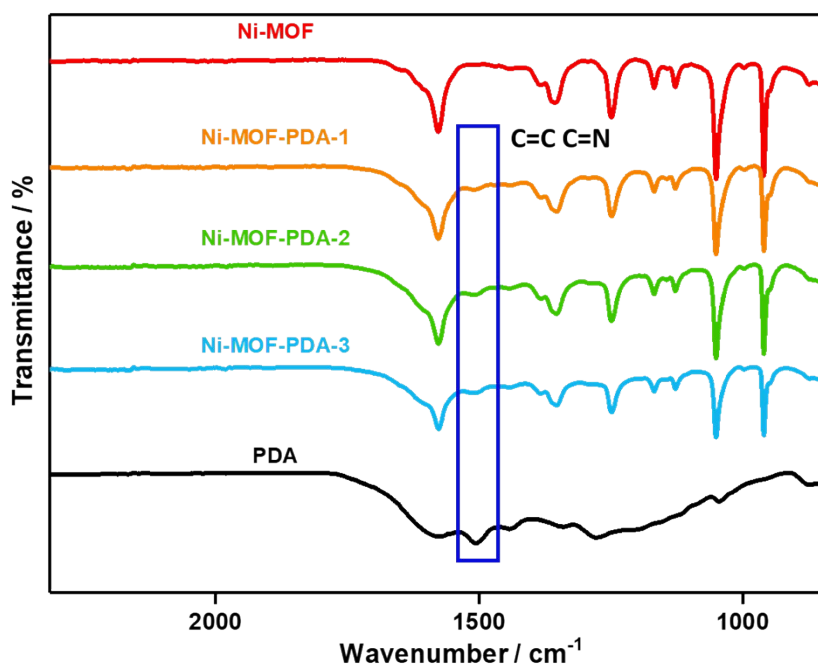


Fig. S4 FTIR spectrum of Ni-MOF (red), Ni-MOF-PDA-1 (orange), Ni-MOF-PDA-2 (green), Ni-MOF-PDA-3 (cyan) and PDA (black).

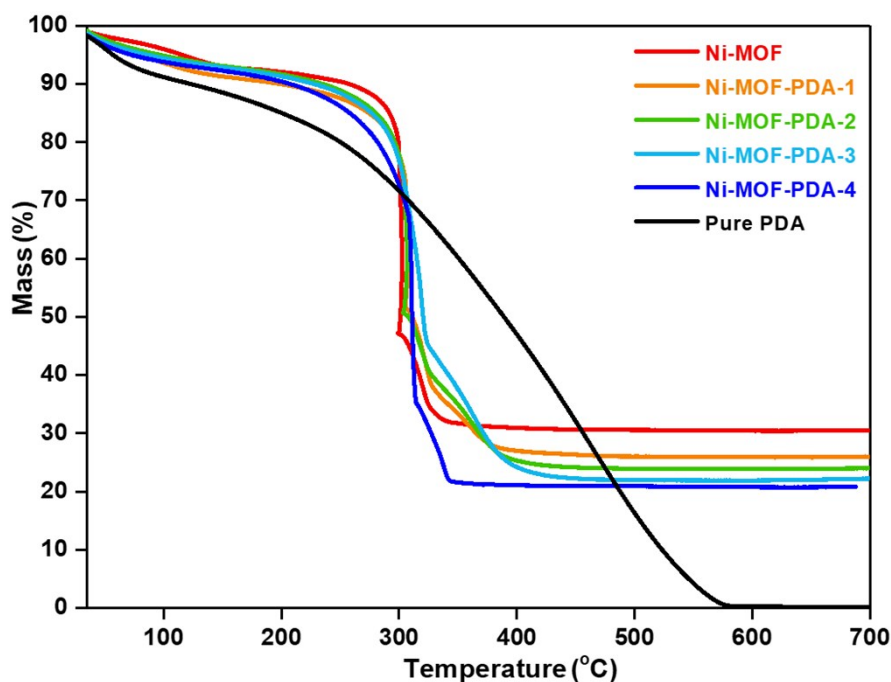


Fig. S5 TGA curve of Ni-MOF (red), Ni-MOF-PDA-1 (orange), Ni-MOF-PDA-2 (green), Ni-MOF-PDA-3 (cyan), Ni-MOF-PDA-4 (blue) and pure PDA (black).

Note: As shown in Fig.S5, all of the PDA residuals are gone at 575 °C due to the evolution of gas when the polymer decomposes; however, the Ni-MOF decomposes to form nickel oxide. From the TGA data, we calculate a 30.4 mass % of NiO remains. This means that 0.304 g of residual NiO will result from one gram of Ni-MOF. However, we expect the composite to yield less residual NiO due to the added polymer. As shown in the Fig. S5 indeed this is the case as the weight of residual NiO from the composites are calculated to be 0.260 g, 0.240 g, 0.212 g, 0.207 g NiO per gram of Ni-MOF-PDA-1, Ni-MOF-PDA-2, Ni-MOF-PDA-3 and Ni-MOF-PDA-4, respectively. Using the following equation we can then calculate the mass % of Ni-MOF (x): $(0.304(x))/100 = 0.260, 0.240, 0.212, \text{ or } 0.207$. From this equation we learn that the mass percent of starting Ni-MOF in each composite is 85.5, 78.9, 69.8, and 68.1 for Ni-MOF-PDA-1, Ni-MOF-PDA-2, Ni-MOF-PDA-3 and Ni-MOF-PDA-4, respectively. Then we used the following equation to calculate the percent dopamine = 100-x. So, the PDA weight percent in Ni-MOF-PDA-1, Ni-MOF-PDA-2, Ni-MOF-PDA-3 and Ni-MOF-PDA-4 are ~14.5 wt%, 21.1 wt%, 30.2 wt% and 31.9 wt%, respectively. Please see Figure S5 in the revised supporting information, where we have added the above description. It should be noted that we also did combustion analysis to obtain the percent N. This also gives us an estimate of the polymer loading which correlates well with the calculations from the TGA. The results obtained for Ni-MOF-PDA-1, Ni-MOF-PDA-2, and Ni-MOF-PDA3 were 15.9%, 22.4%, and 28.2%. Please see Table S1. These values correlate relatively well with the TGA results.

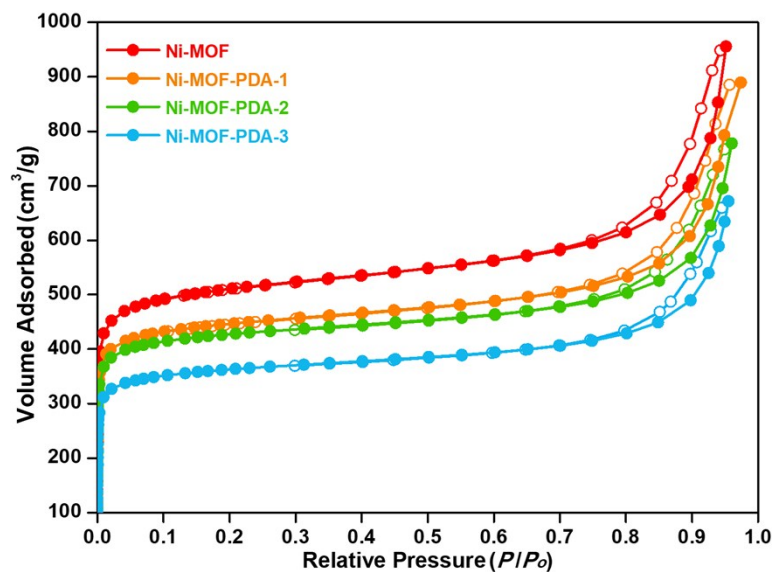


Fig. S6 N₂ adsorption-desorption isotherms of Ni-MOF (red), Ni-MOF-PDA-1 (orange), Ni-MOF-PDA-2 (green) and Ni-MOF-PDA-3 (cyan).

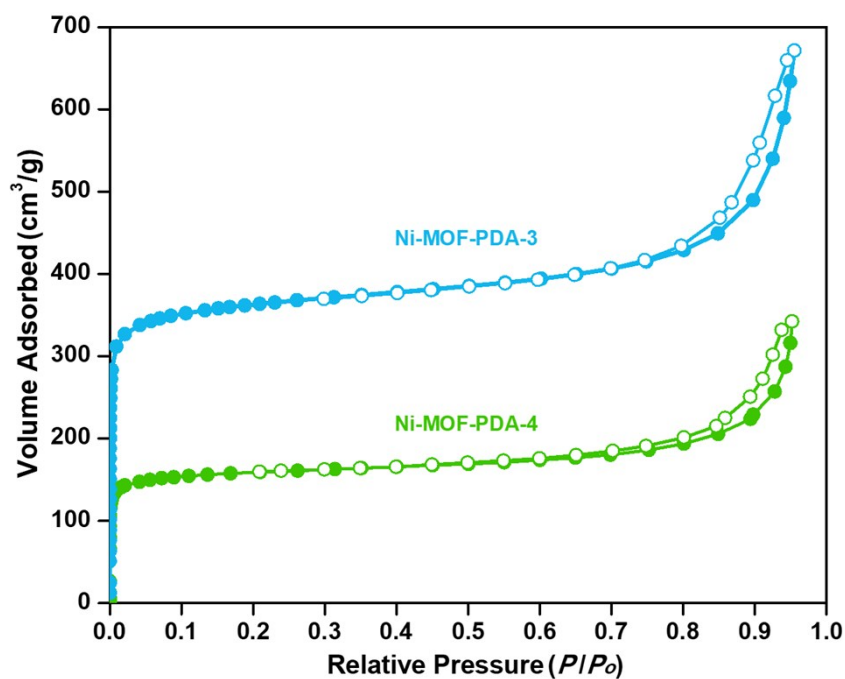
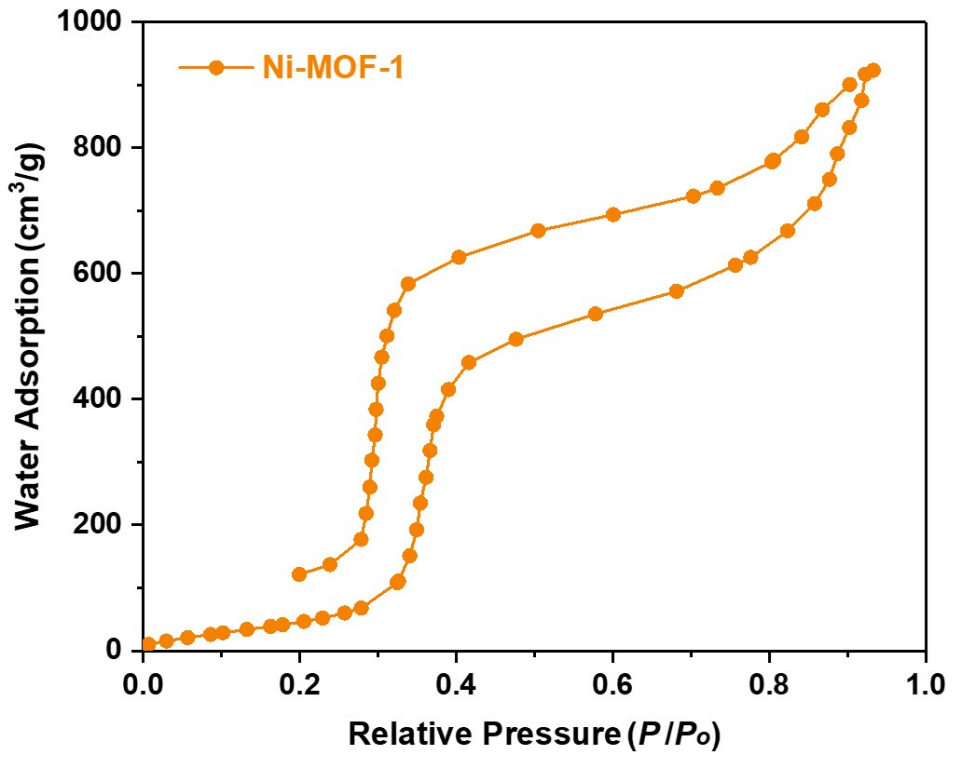
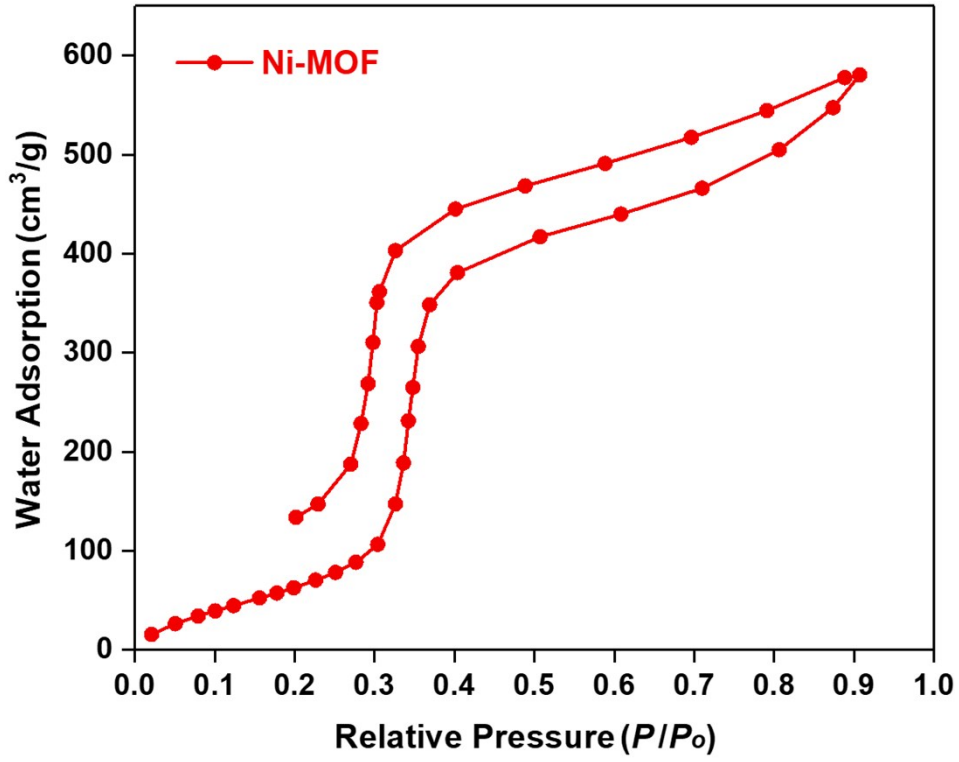


Fig. S7 N₂ adsorption-desorption isotherms of Ni-MOF-PDA-3 (cyan, BET surface area: 1408 m²/g) and Ni-MOF-PDA-4 (green, BET surface area: 621 m²/g) where the PDA loading is 30.2 and 31.8 wt% respectively.



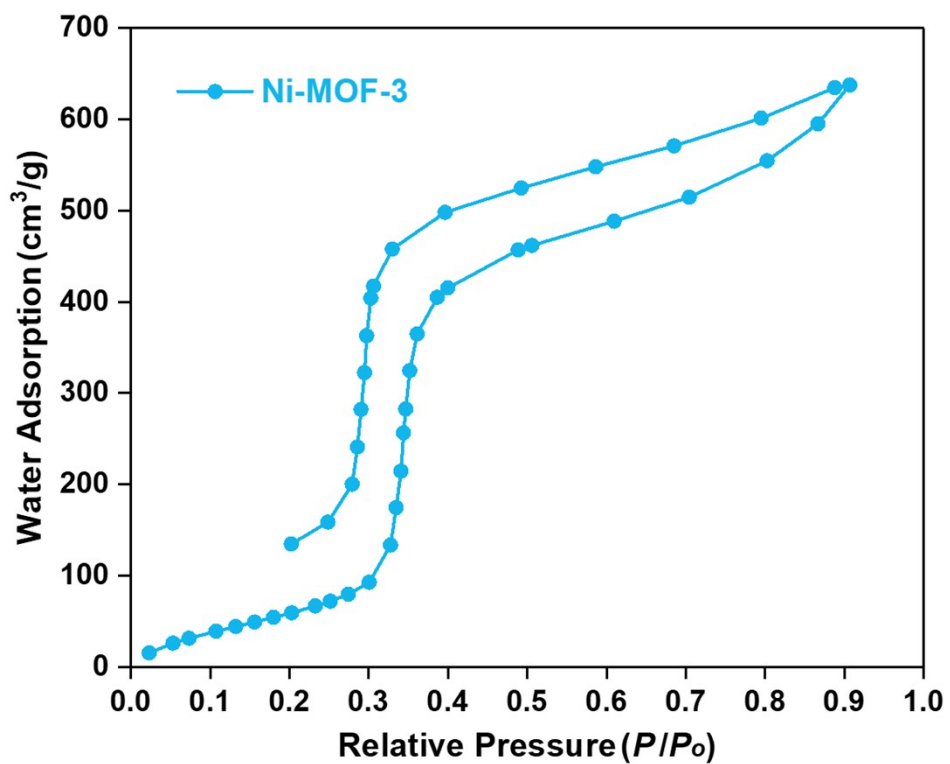
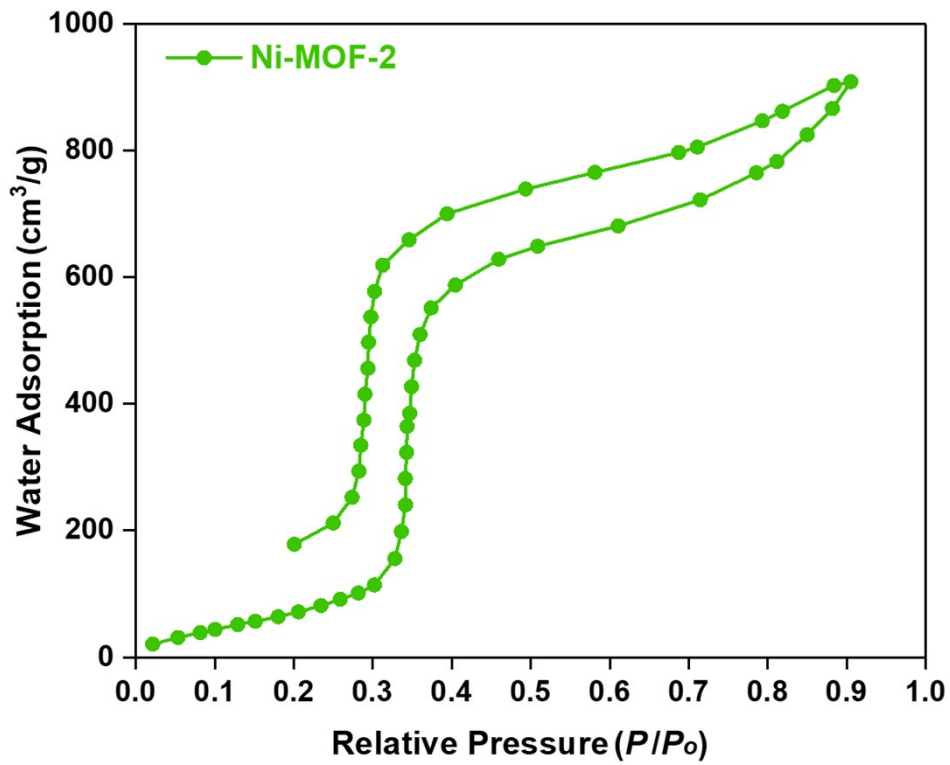


Fig. S8 Water vapor sorption isotherm of Ni-MOF (red), Ni-MOF-PDA-1 (orange), Ni-MOF-PDA-2 (green) and Ni-MOF-PDA-3 (cyan) measured at 298 K.

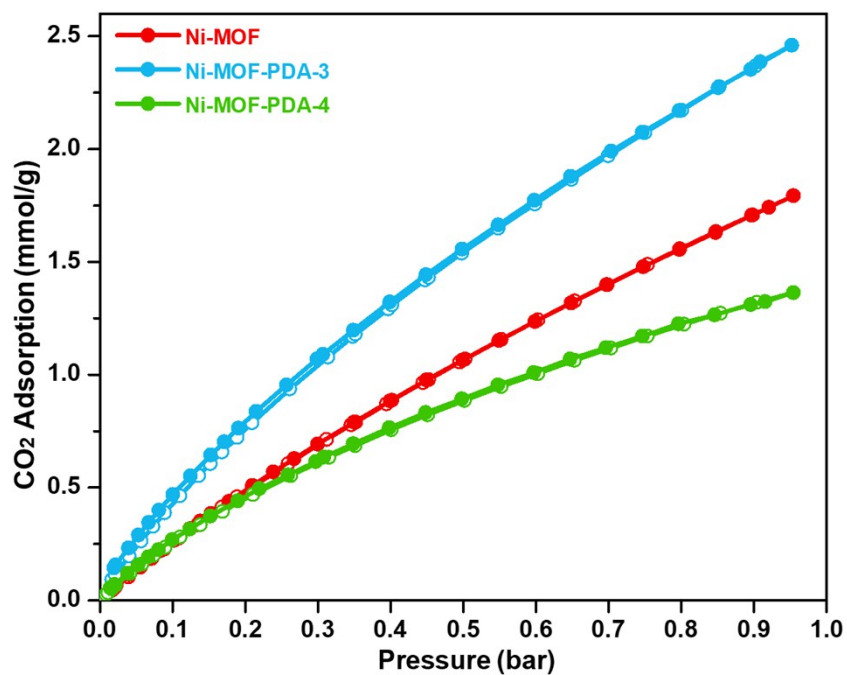


Fig. S9 CO₂ isotherms of Ni-MOF (red), Ni-MOF-PDA-3 (cyan) and Ni-MOF-PDA-4 (green).

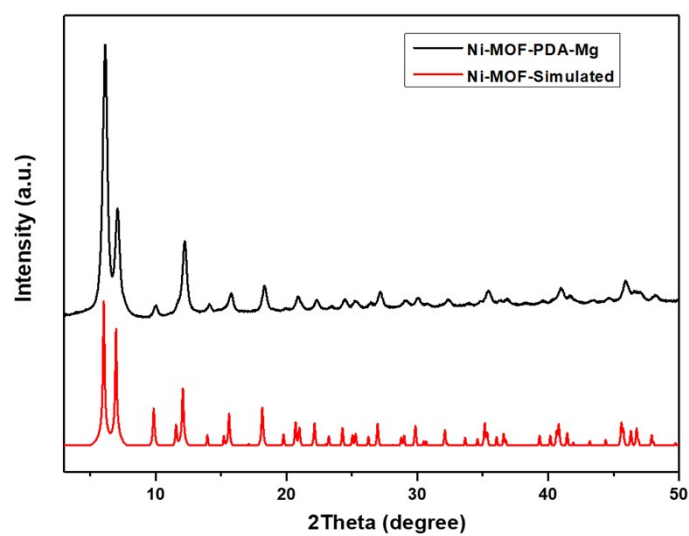


Fig. S10 XRD patterns of simulated Ni-MOF (red) and as-synthesized Ni-MOF-PDA-Mg (black). ($\lambda=1.5418 \text{ \AA}$)

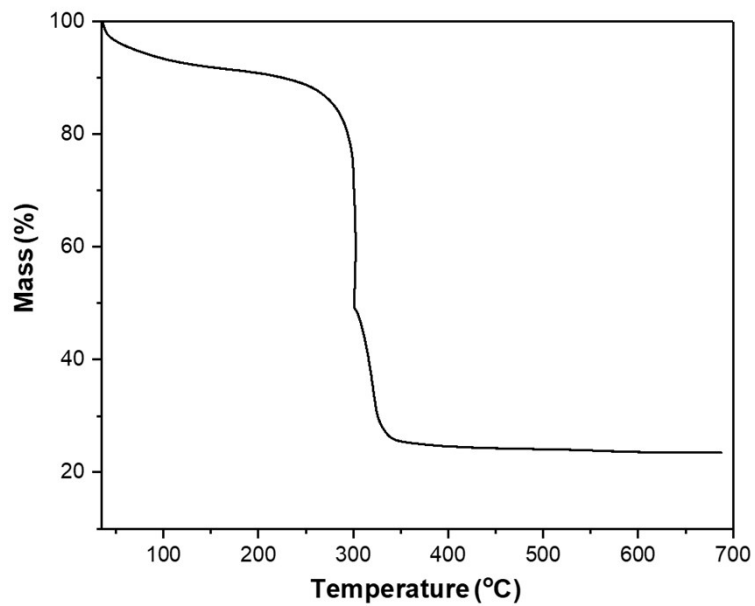


Fig. S11 TGA analysis of Ni-MOF-PDA-Mg.

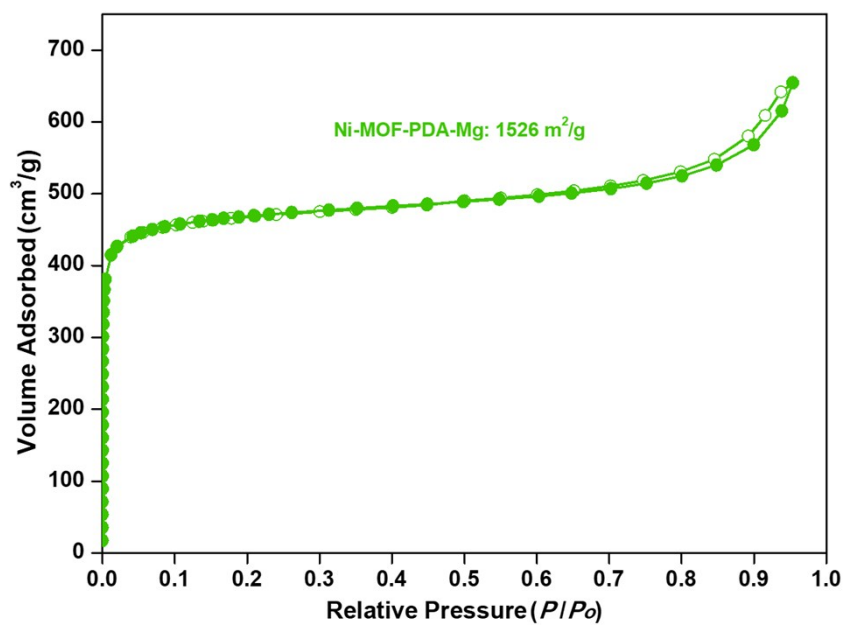
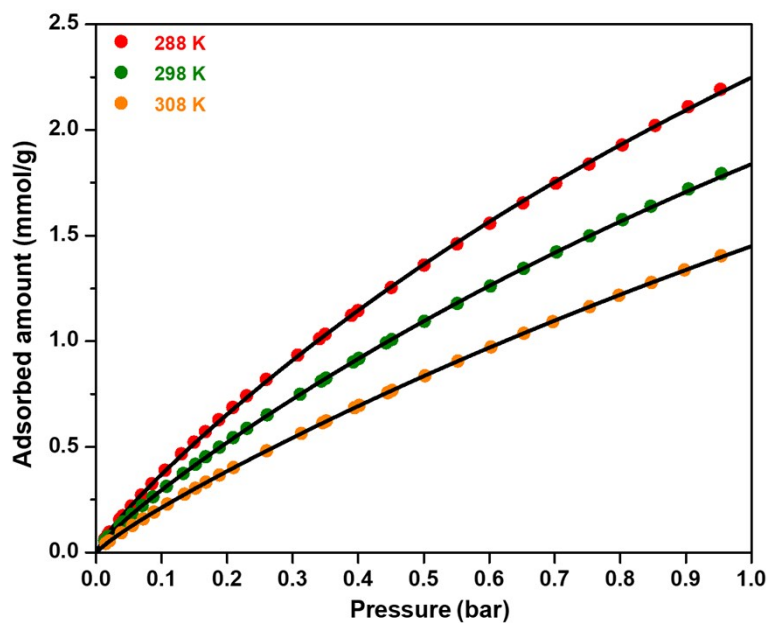
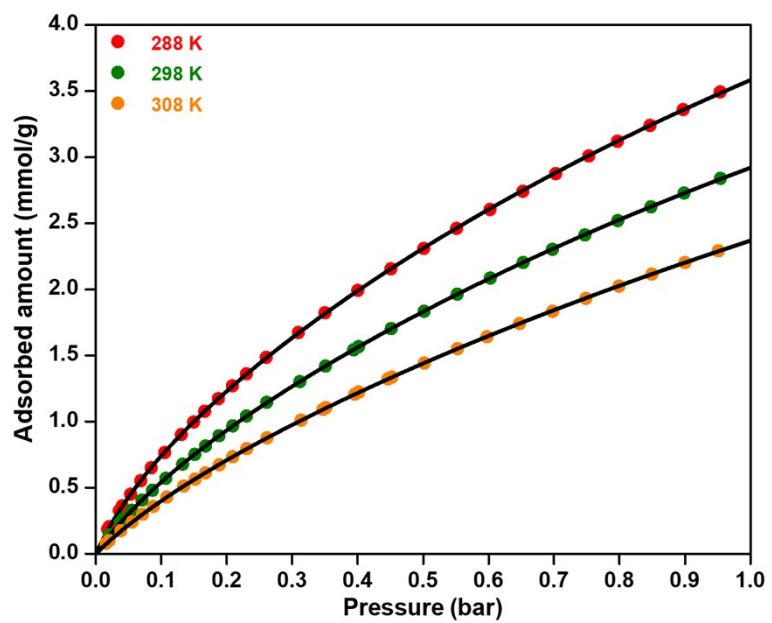


Fig. S12 N₂ adsorption-desorption isotherms of Ni-MOF-PDA-Mg.

A:



B:



C:

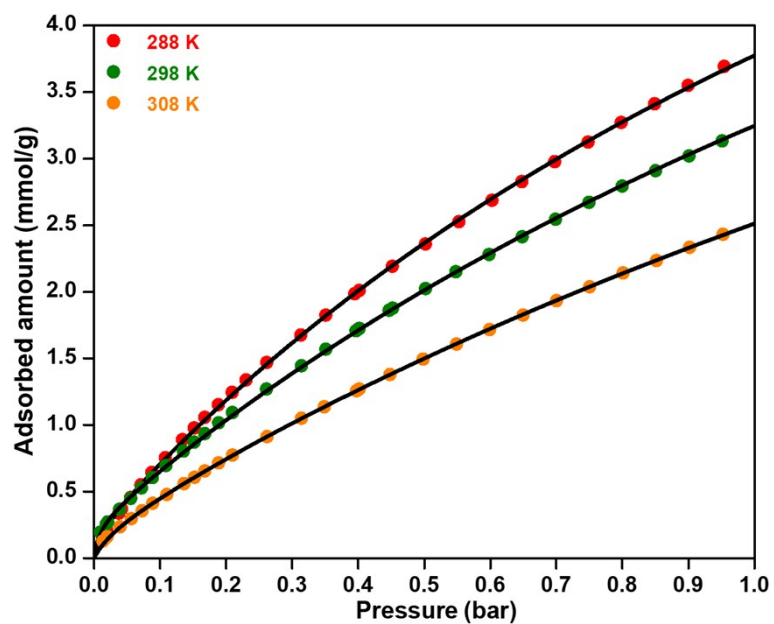


Fig. S13 Experimental CO₂ adsorption isotherms (dot) and the fitted data (line) using dual-site Langmuir model for Ni-MOF (A), Ni-MOF-PDA-3 (B) and Ni-MOF-PDA-Mg (C).

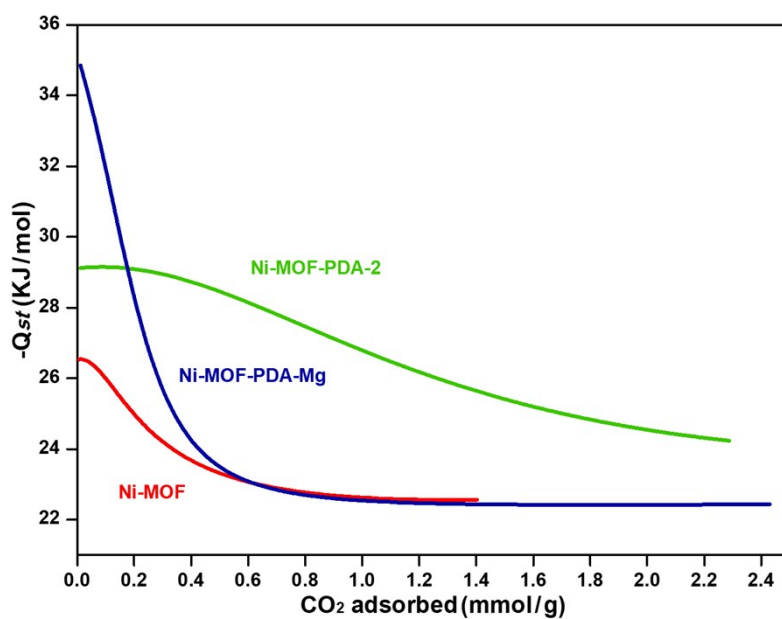


Fig. S14 Isothermic heat of Ni-MOF (red), Ni-MOF-PDA-2 (green), and Ni-MOF-PDA-Mg (royal blue).

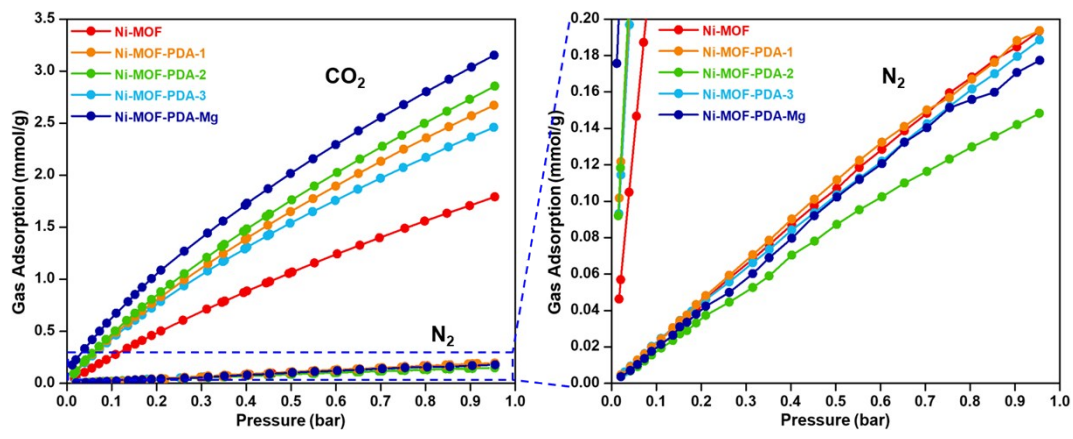
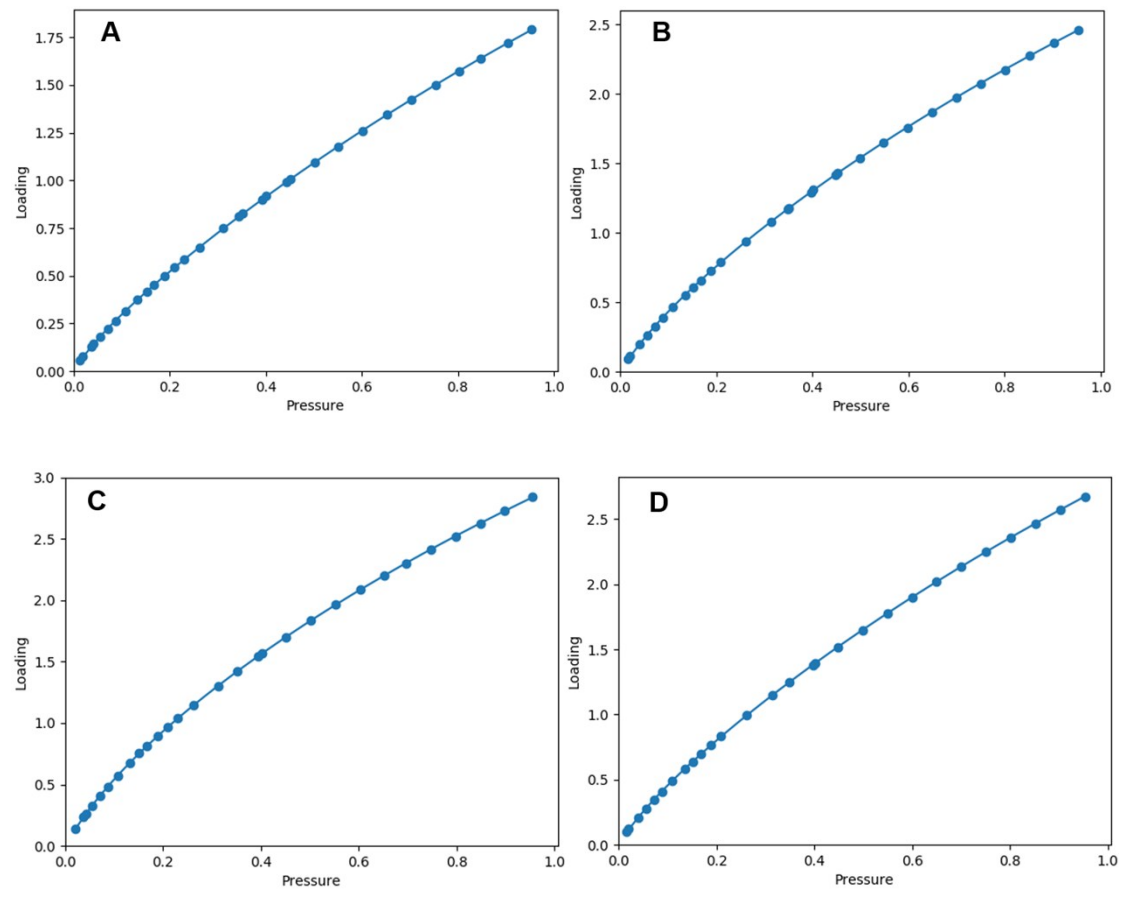


Fig. S15 Selective adsorption of CO₂ over N₂ adsorption at 298 K of Ni-MOF (red), Ni-MOF-PDA-1 (orange), Ni-MOF-PDA-2 (green), Ni-MOF-PDA-3 (cyan) and Ni-MOF-PDA-Mg (royal blue).



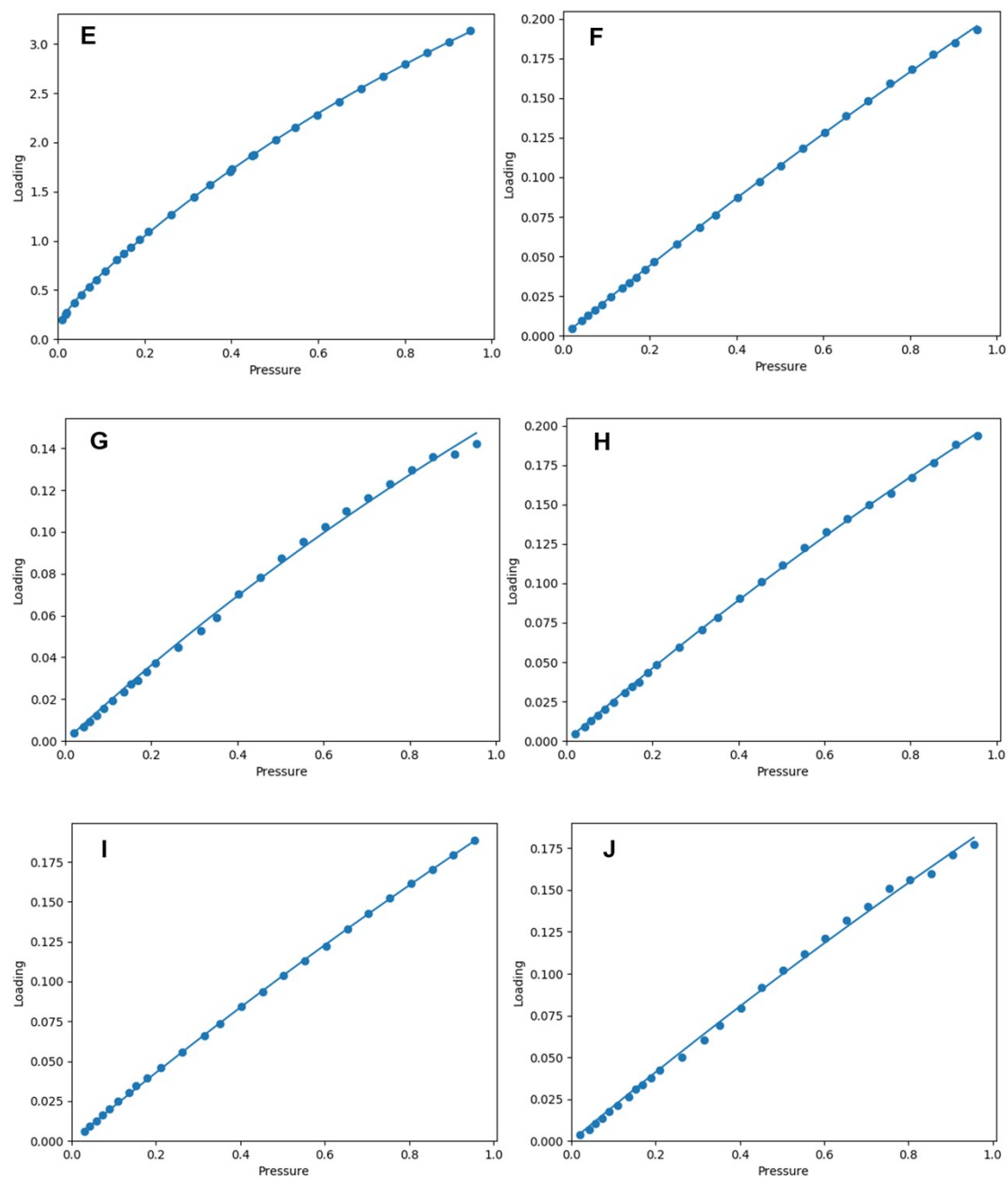


Fig. S16 Experimental CO₂ adsorption isotherms (dot) and the fitted data (line) using single-site Langmuir model for Ni-MOF (A), Ni-MOF-PDA-1 (B), Ni-MOF-PDA-2 (C), Ni-MOF-PDA-3 (D) and Ni-MOF-PDA-Mg (E). Experimental N₂ adsorption isotherms (dot) and the fitted data (line) using single-site Langmuir model for Ni-MOF (F), Ni-MOF-PDA-1 (G), Ni-MOF-PDA-2 (H), Ni-MOF-PDA-3 (I) and Ni-MOF-PDA-Mg (J).

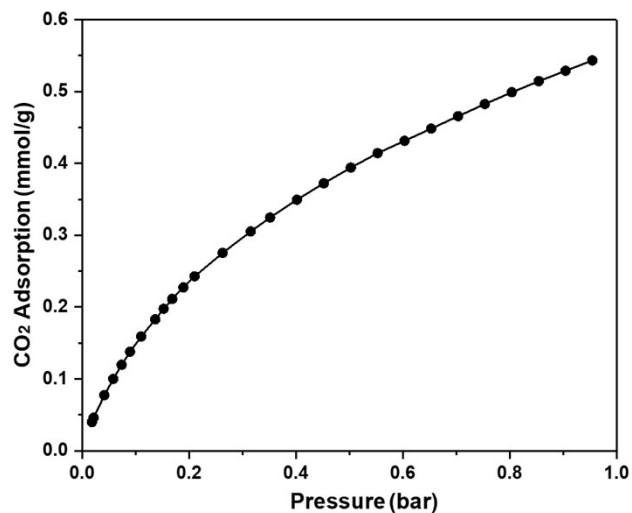


Fig. S17 CO₂ adsorption of bulk PDA at 298 K.

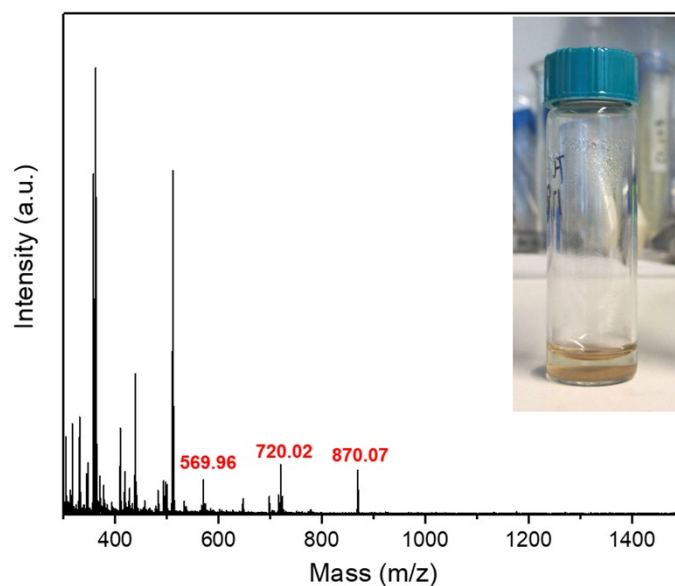


Fig. S18 MALDI-TOF-MS spectra of Ni-MOF-PDA-2. The sample was destroyed in 4.0 M HCl.

Note: The MALDI-TOF spectra result showed that PDA consists of as many as 5 monomeric units (Fig. S18), that are also complexed with Ni²⁺. It should be noted that there are larger units remaining in the polydopamine sample, as we were unable to digest some of the material.

Table S1. Elemental analysis results for Ni-MOF, Ni-MOF-PDA-1, Ni-MOF-PDA-2 and Ni-MOF-PDA-3. The weight percentage of polydopamine was calculated based on the N%.

Samples	C%	N%	H%	PDA%
Ni-MOF	47.04	16.73	3.27	0
Ni-MOF-PDA-1	50.01	15.59	3.18	15.9
Ni-MOF-PDA-2	51.23	15.13	3.15	22.4
Ni-MOF-PDA-3	52.32	14.72	3.12	28.2

Table S2. Fitted parameters for CO₂ adsorption isotherms at different temperature of Ni-MOF (A), Ni-MOF-PDA-3 (B) and Ni-MOF-PDA-Mg (C).

Samples	$q_{sat,1}$	b_1	$q_{sat,2}$	b_2
Ni-MOF (288 K)	0.095	0.030	7.000	0.00044
Ni-MOF (298 K)	0.085	0.029	6.501	0.00037
Ni-MOF (308 K)	0.063	0.018	6.501	0.00027
Ni-MOF-PDA-3 (288 K)	0.684	0.009	9.857	0.00043
Ni-MOF-PDA-3 (298 K)	0.502	0.007	9.031	0.00038
Ni-MOF-PDA-3 (308 K)	0.392	0.006	8.906	0.00030
Ni-MOF-PDA-Mg (288 K)	0.202	0.098	10.196	0.00054
Ni-MOF-PDA-Mg (298 K)	0.266	0.120	10.083	0.00042
Ni-MOF-PDA-Mg (308 K)	0.204	0.032	10.079	0.00030

Table S3. The IAST predicted selectivity toward CO₂ vs N₂ for fuel gas CO₂/N₂ mixtures (CO₂ : N₂ = 85 : 15) on the samples at 298 K of Ni-MOF before and after loading PDA.

Materials	IAST predicted selectivity of CO ₂ vs N ₂ (85:15)
Ni-MOF	16.0
Ni-MOF-PDA-1	25.7
Ni-MOF-PDA-2	58.7
Ni-MOF-PDA-3	27.5
Ni-MOF-PDA-Mg	58.9

Table S4. Fitted parameters for CO₂ adsorption isotherms and N₂ adsorption isotherms for calculating selectivity of Ni-MOF, Ni-MOF-PDA-1, Ni-MOF-PDA-2, Ni-MOF-PDA-3 and Ni-MOF-PDA-Mg at 298 K.

Samples	q _{sat,1,CO2}	b _{1,CO2}	q _{sat,2,CO2}	b _{2,CO2}	q _{sat,N2}	b _{N2}
Ni-MOF	0.136	14.956	7.658	0.291	2.035	0.111
Ni-MOF-PDA-1	0.329	7.820	9.321	0.318	1.366	0.175
Ni-MOF-PDA-2	0.521	7.201	9.241	0.363	0.779	0.244
Ni-MOF-PDA-3	0.256	10.597	10.624	0.313	1.868	0.117
Ni-MOF-PDA-Mg	0.266	108.630	9.437	0.457	1.882	0.112

References:

- 1) T. Li, D. -L. Chen, J. E. Sullivan, M. T.; Kozlowski, J. Karl Johnson and N. L. Rosi, *Chem. Sci.* 2013, **4**, 1746-1755.
- 2) J. A. Mason, K. Sumida, Z. R. Herm, R. Krishna and J. R. Long, *Energy Environ. Sci.* 2011, **4**, 3030-3040.
- 3) P. Mishra, H. P. Uppara, B. Mandal and S. Gumma, *Ind. Eng. Chem. Res.* 2014, **53**, 19747-19753.
- 4) J. M. Huck, L. Lin, A. H. Berger, M. Niknam Shahrak, R. L. Martin, A. S. Bhowan, M. Haranczyk, K. Reuter and B. Smit, *Energy Environ. Sci.* 2014, **7**, 4132-4146.
- 5) C. M. Simon, B. Smit and M. Haranczyk, *Comput. Phys. Commun.* 2016, **200**, 364-380.